CHAPTER IV

PROBING HOST-GUEST INCLUSION COMPLEXES OF AMBROXOL HYDROCHLORIDE WITH α- & β-CYCLODEXTRINS BY PHYSICOCHEMICAL CONTRIVANCE SUBSEQUENTLY OPTIMIZED BY MOLECULAR MODELING SIMULATIONS

ABSTRACT

Herein, we report the inclusion of AMB in cyclodextrins leading to host-guest assemblies. The inclusion complexes comprised of Ambroxol Hydrochloride (AMB) with α-cyclodextrin (αCD) and β-cyclodextrin (βCD) have been confirmed by experimental (UV-vis titration, FTIR, ESI-MS, ^{1}NMR, 2D-NMR) and computational studies (molecular docking, molecular mechanics calculation). The molecular docking studies demonstrate a better insight into geometry and inclusion mode of AMB inside αCD as well as βCD cavity. Formation of inclusion complexes with different cyclodextrins causes some structural changes of guest molecules during the encapsulation process confirmed by bond length, dihedral angle changes and dynamic simulations.

Keywords: α-cyclodextrin, β-cyclodextrin, conformational change, supramolecular assembly, host-guest dynamics.

1. INTRODUCTION

Now-a-days, site specific formulation of a potential drug is very much important for the betterment of the drug in pharmaceutical industry [1]. Although, Ambroxol Hydrochloride (AMB) is a mucolytic drug that reduces the thickness of the sputum [2] and also used to treat conditions with abnormal mucus secretion [3] allowing the patient to breathe freely and deeply by promoting mucus clearance, facilating expectoration and easing productive cough [4,5]. But being soluble in hot water and practically insoluble in dichloro methane and soluble in Methanol [6], a

supramolecular assemble of pure Ambroxol Hydrochloride (AMB) with cyclodextrin molecules tagged with a protein or enzyme could make it a potent mucolytic and mucokinetic agent. Some recent studies include the drugs having a role in treatment of Gaucher's disease [7], Parkinson disease [8] and other aging-associated diseases involving dysfunction of autophagy [9].

AMB is a mucolytic drug as a salt form of Ambroxol (Scheme 1), a metabolite of bromohexine [10]. Ambroxol can also be used as a pharmacological chaperone therapy (PCT) for the treatment of Guacher Disease (GD) [11]. Ambroxol Hydrochloride occurs as a white crystalline powder [12]. Due to its poor water solubility, AMB has been used as an oral suspension. The aqueous solubility and dissolution of these drugs are key factors in determining the bioavailability of its oral preparation [13].

Cyclodextrins (CD) are cyclic oligosaccharides widely used for the recognition of various guest molecules give rise to inclusion complex (IC) [14]. CDs are non toxic, biodegradable and biocompatible along with the collective effects of inclusion, size-specificity, controlled release capability and transport properties make it suitable as a host molecule [15,16]. Supramolecular complexation can increase the water solubility as well as bio availability [17,18]. Among different types of cyclodextrins, αCD and βCD (Scheme 1) are taken as host molecules due to both size and solubility matching with the Ambroxol Hydrochloride i.e the guest molecule. Now-a-days, apart from experiments, researchers also perform different molecular simulation studies with guest, host and their inclusion complexes to gather information at a molecular level e.g, quantum mechanics, molecular dynamics (MD) and molecular mechanics (MM) approximations [19,20].

The aim of the present study is to evaluate whether host-guest inclusion complex has been formed between the guest Ambroxol Hydrochloride and the two types of hosts cyclodextrins αCD and βCD and also to investigate the different interactions between host and the guest molecules in the inclusion complex. Additionally, molecular modeling study by MOE.2015 software from chemical

computing group was performed to validate the change in geometrical configuration of the complex obtained from experimental results [21]. Different physiochemical, spectroscopic techniques for the two inclusion complexes in aqueous solution have been performed to investigate whether the IC formation has taken place as well as to study different interactive forces occurring in the two inclusion complexes.

2. EXPERIMENTAL SECTION

2.1 Materials and Materials.

Ambroxol Hydrochloride (M.W=414.57, Purity>98.0%) which was used as the guest molecule in our study was purchased from TCI Chemicals (India) Pvt. Ltd & the two hosts required that is βCD (M.W=1134.98, Purity >97.0%) and αCD (M.W=972.84, Purity >98.0%) were bought from SIGMA- ALDRICH India (Table S1). Double distilled water has been used throughout the experiment.

2.2 Methods.

Stock solutions of Ambroxol Hydrochloride, βCD and αCD were prepared by mass (Mettler Toledo AG-285 with uncertainty 0.0001 g) and by dilution. The solution of αCD and βCD were prepared by heating it slightly in a water bath. All the ^{1}H-NMR and 2D-NMR data were plotted with the help of Mestrenova 12. Origin 2018 software has been used for the plotting the entire graphs. All the spectroscopic experiments were carried out in a solution of ethanol/water mixture (3:7, v/v).

2.3 UV–visible spectroscopy.

UV-vis titration was performed by using Agilent 8453 Spectrophotometer. The temperatures were regulated with a digital thermostat for the association constant measurement. The absorption spectra were recorded at 293±0.15K, 303±0.15K, 313±0.15K respectively.

2.4 Fourier transform infrared (FTIR).

FTIR spectra were recorded by a Perkin Elmer FTIR spectrometer by the solid KBr disk technique. KBr disks with 1 mg of solid inclusion complex and 100 mg

of KBr were prepared. Measurements were performed in the scanning range of (4000–400 cm^{-1}) at the room temperature to record the FT-IR spectral data.

2.5 ^{1}H-NMR and 2D-NMR Spectroscopy.

All NMR spectra were recorded on a Bruker AVANCE spectrometer at 400 MHz and 25 ^{0}C in D_2O. The residual HDO line had a line width at a half-height of 2.59 Hz. Two-dimensional (2D) ROESY spectra were acquired at 25 ^{0}C with number of scan 8, and a 2048 K time domain in F2 (FID resolution 5.87 Hz) and 460 experiments in F1.

2.6 ESI-MS spectrometry.

ESI-MS spectra for the both complexes were collected using Agilent, 6460 Triple quad LC/MS, 1200 Infinity series equipped with electrospray ionization (ESI) interface. The gas temperature was 300 ^{0}C with flow rate of 5 L min^{-1}. The capillary voltage was calibrated at 3.5 kV and injection volume was about 5.00 ml.

2.7 Molecular Modeling Studies.

Molecular modeling studies were performed to predict the formation of AMB+αCD and AMB+βCD inclusion complexes and to measure their binding affinity by utilizing MOE.2015 software, which are available in the Chemical Computing Group (CCG). The 3D optimized structure of AMB (ID: 234307), αCD (ID: 125105), βCD (ID: 762697) were taken from Chembridge Crystal data centre (CCDC) as CIF file and used as received. Hydrogen atoms and partial charges were added to the protein. Molecular modeling calculations were carried out with molecular mechanics MMFF94x force field. The hydrogens and charges were fixed, and the RMS gradient was set to 0.005 kcal/mol. Conformations of ligand (CDs) were fitted in the position with the Triangle Matcher method and ordered with the London ΔG scoring function. A maximum of 5 conformations of each guest were allowed to be saved in a separate database file as .mdb format. The produced poses were ranked based on their docking scores. Finally, we choose the best energy pose [22,23].

2.8 Dynamic Simulation.

Molecular dynamics and simulations studies are generally performed to obtain the stable structure of inclusion complexes with respect to time, temperature, kinetic energy and potential energy. The forcefield was taken to be MMFF94x. MOE dynamics simulation uses the Nosé-Poincaré-Andersen (NPA) equations of motion. Default steps and protocols of the MD were selected to optimize the systems equilibrium 100 ps and production run was carried out for 500 ps.

2.9 Sample preparation of Solid Inclusion Complex of Ambroxol Hydrochloride with Cyclodextrins.

To prepare 1:1 a solid Inclusion Complex between Ambroxol Hydrochloride and αCD as well as with βCD, at first, 30 mg of solid guest compound of AMB (which is also pretty much soluble in hot water) was taken in a beaker and amount 40ml of distilled water was added to it and placing it in a thermostated water bath at temperature set at 323.15K with constant stirring in a magnetic stirrer. Next, accurately measured 70.39 mg of αCD and 82.13 mg of βCD were added in solid form in two different beakers slowly in presence of the constant stirring. It was kept in the thermostated water bath for 24-48 hours. Thereafter, it was collected and dried in a hot oven & after that inclusion complexes in the solid form were obtained.

3. RESULTS AND DISCUSSIONS.

Ambroxol Hydrochloride guest molecule selected in this investigation was moderately soluble in water. Our aim was to study the formation of inclusion complex between the host and the guest and also to evaluate the interactions and different thermodynamic parameters of the inclusion complex, so all the measurements were done in room temperature and in aqueous-ethanolic solution such as UV-vis Studies etc. However, FTIR Spectroscopy, NMR, SEM analysis were performed by the prepared solid inclusion complex between Ambroxol Hydrochloride and CDs.

3.1. Job's plot: Determination of Stoichiometry behaviour of Cyclodextrins Inclusion Complex with Ambroxol Hydrochloride.

Job's plot method which is also known as the continuous variation method is a very efficient and successful way to recognize stoichiometry of any host-guest inclusion complexes [24]. So, due to this reason the Job's Plot was applied here by using UV-visible spectroscopy. Here, two sets of solutions were prepared of Ambroxol Hydrochloride with αCD and βCD respectively in 30% ethanolic-aqueous (3:7, v/v) solution, by varying the mole fractions of the guest (Ambroxol) in the range of 0-1. Job's plots of the mentioned sets of solutions were plotted as ΔA×R against R, where ΔA means the difference in absorbance of AMB (Guest) without and with CD and R=[AMB]/([AMB]+[CD]). The absorbance values were obtained at respective λ_{max} for each solution by maintaining 298.15 K temperature. The stoichiometry of an inclusion complex is obtained by taking the corresponding value of R at the maximum point on the Job's Plot curve, for example, if the ratio of guest to host is 1:2 for R∽0.33, 1:1 for R∽0.5 and 2:1 for R∽0.66 and so on. Here, in this work we got R∽0.5 as maxima in the plot (Fig. 1), reflecting a 1:1 stoichiometry (Guest:Host) for both the inclusion complexes (Table S2 & S3).

3.2. Determination of binding constant of both complexes in aqueous ethanol by UV–vis spectroscopy.

The binding constant between αCD, βCD and the guest molecule Ambroxol has been calculated via UV–Vis spectroscopy with the help of Benesi–Hildebrand technique which represents one of the most well-known strategies to determine binding constants of the Inclusion Complexes based on absorption spectra of the inclusion complex [25]. Accurate estimation of binding (association) constants of the inclusion complexes under investigation can be obtained by observing changes in the absorption intensity of the AMB at different temperature as a function of the CD's concentration (Table 2) and according to method for 1:1 Inclusion complex between guest and host, the double reciprocal plots have been drawn using equation (1).

$$\frac{1}{[A-A_o]} = \frac{1}{K_a[AMB]_o\Delta\varepsilon} \times \frac{1}{[CD]_o} + \frac{1}{\Delta\varepsilon} \quad \text{..... (1)}$$

For AMB+αCD, Association constant of 1:1 host and guest was found to be 4226 M^{-1}, 8993 M^{-1}, and 15799 M^{-1} at 293.15K, 303.15K and 313.15K respectively with good correlation factors (Table 1 & Table S4). Double reciprocal plot was calculated using Benesi-Hildebrand to obtain the slope and intercept (Fig. S1, S2 & S3).

Association constant (k_a) value for AMB+βCD was calculated by dividing the intercept by the slope of the straight line (Table S6), which was found from the double reciprocal plot (Figure S5, S6, S7) at three different temperatures 293.15K , 303.15K & 313.15K have been found to be 27780 M^{-1}, 37333 M^{-1} & 45379 M^{-1} respectively (Table 1).

From Table 1, we observe that with the increase in temperature association constant values (Ka) increases for both the system and the Ka values for AMB with βCD system were found to be higher in all three temperatures than the AMB with αCD system. The linear increase in k_a value when increasing the temperature from 293.15K to 313.15K clearly indicated the endothermic nature of Inclusion Complexation between Ambroxol Hydrochloride and αCD and βCD and also suggests that βCD forms the complex with better stability.

3.3 Thermodynamic parameters:

The thermodynamic parameters of the analyzed inclusion processes, enthalpy change (ΔH°) and entropy change (ΔS°) and Gibbs free energy change (ΔG°) can be obtained by means of the classical van't Hoff equation (eqn. 2) [26]:

$$\Delta G° = \Delta H° - T\Delta S° \quad \text{..... (2)}$$

In case of AMB+αCD inclusion complex (Table 2), ΔG° was found to be -4.86 Kcal/mol, -5.44 Kcal/mol, and -6.01 Kcal/mol at 293.15K, 303.15K and 313.15K respectively (Table S5).

However, in case of AMB+βCD inclusion complex, ΔG° was found to be -5.96 Kcal/mol, -6.31 Kcal/mol, and -6.91 Kcal/mol at 293.15K, 303.15K and 313.15K respectively (Table 2 & S7). In both cases, the ΔH° and ΔS° are found to be positive. These values indicate that the inclusion processes are endothermic in nature (entropically favored, and with a nonfavorable enthalpic expression). Thus, these results indicate hydrophobic effects are the main driving forces for the formation of inclusion complexes. In order to approve the above experimental results, a molecular modeling study combining MD simulations was performed.

3.4. FTIR spectral analysis:

FTIR spectroscopy is an important method to confirm the formation of inclusion complex from the variation in shape, size, shift and intensity of the absorption peak of Guest and Host moiety [27]. There will be broadening, widening, disappearance or change in intensity of the peaks due to complexations [28]. The FTIR spectra of pure AMB, αCD, βCD and the inclusion complexes AMB+αCD and AMB+βCD were recorded and all the peaks were assigned and shown in Fig. 4 & 5.

The infrared spectra of the guest molecule (AMB) showed some few characteristic peaks e.g, a peak at 3193 cm^{-1} was associated with the stretching vibration of aromatic C-H bond [29]. The strong C=C stretching vibrational peak was observed at 1629 cm^{-1}, which belongs to the benzene ring [30]. Usually, the vibration of aromatic C-N in NH_2 group observed at 1284 cm^{-1}. The aliphatic C-N stretching mode was observed at 1458 cm^{-1}. The N-H of aromatic amine group showed its stretching vibration at 3300 cm^{-1}. However, symmetric stretching mode of aliphatic amine N-H appeared at 3284 cm^{-1} [31].

When inclusion complex is formed, some of the characteristic peaks got disappeared. There are significant differences in the spectra of the inclusion complexes in comparison with the individual drugs. Most of the peaks of the drugs get flattened, indicating a strong intermolecular interaction between the drugs and CDs [32].

For AMB+αCD inclusion complex, the protons belong to the aromatic ring which appeared at 3193 cm^{-1} in pure AMB is diminished in the IR spectra of the complexes. The vibration of aromatic C-N in NH_2 group observed at 1284 cm^{-1} and C-N in -NH- group at 1458 cm^{-1} (Fig. 4) has been disappeared possibly due to formation of encapsulation. Therefore, it suggests that probably few portions of the aromatic part of AMB as well as cyclohexyl part have been encapsulated to the αCD cavity.

For AMB+βCD inclusion complex, the aromatic ring proton which appeared at 3193 cm^{-1} in pure AMB is also diminished in the IR spectra of the complexes (Fig. 5). The vibration of aromatic C-N in NH_2 group observed at 1284 cm^{-1} has been shifted to 1206 cm^{-1} whereas, C-N in -NH- group observed at 1458 cm^{-1} has been shifted to 1447 cm^{-1} possibly due to formation of encapsulation. Therefore, it suggests that probably few portions of the aromatic part of AMB as well as cyclohexyl part have been encapsulated to the cyclodextrin cavity.

3.5. ^{1}H-NMR Spectra analysis.

The molecular interactions between Host-Guest molecules in inclusion complexes are investigated using ^{1}H NMR [33]. Normally, ^{1}H NMR is used for obtaining the molecular interaction information regarding selective line broadening or chemical shift displacement of host and guest molecules. These chemical shifts are easily observable for protons located at the inner surface (H-3 and H-5) of the cyclodextrins, but it is very difficult to observe the chemical shifts of protons (H-1, H-2 & H-4) located at the outer surface of the Cyclodextrin [34]. It can be observed that these chemical shifts appeared due to inclusion complex development due to the inclusion of Guest into the Host molecule and not because of non-specific correlation between host-guest molecules.

The possible interaction between AMB and αCD for inclusion complex formation was investigated by comparing the ^{1}H NMR spectra of AMB, αCD and the AMB+αCD inclusion complex in D_2O (Fig S9). The chemical shifts of βCD protons with or without AMB were compared in (Table 3a). The chemical shift variations

were calculated by the equation: Δ(difference)=Δ(complex)-Δ(free). The positive and negative signs indicate a downfield and upfield shifts, In (Table 3a), upfield shifts are quite evident (-0.04 ppm and -0.01 ppm) observed for the H3' and H5' respectively i.e Protons that are located inside the cavity of βCD. But very little to none upfield shifts can be observed of H4' and H1' protons could be observed for the protons of βCD that are located outside the cavity.

Inclusion mode of AMB+αCD complex can also be characterized by the chemical shift variation of proton of AMB. Aromatic protons which are designated as H4, H6 when form inclusion complexes chemical shift values have been shifted to downfield (Δδ: H4 0.02, H6 0.03) which indicated that they tend to appear outside the cavity. Whereas, H8, H9 protons belong to the benzyl and secondary NH protons shows significant upfield shift as well as cyclohexane ring protons also show quite good upfield shift (Table 3b). This concludes that apart from aromatic part, rest of the part has been totally inserted into the cavity.

Similarly, ^{1}H NMR spectra of AMB, βCD and the AMB+βCD inclusion complex in D_2O were taken to verify the possible interaction between AMB and βCD for inclusion complex (Fig. S10). The chemical shifts of βCD protons with or without AMB were compared in (Table 4a). Upfield shifts are quite obvious observed for the H3' and H5' respectively i.e Protons that are located inside the cavity of βCD. But very little to none upfield shifts can be observed of H4' and H1' protons could be observed for the protons of βCD that are located outside the cavity.

It is known that H5' protons are near the narrow side of the cavity while H3' protons are near the wide side of the cavity of βCD. In our study of AMB+βCD inclusion complex formation, H3' possessed reasonably larger chemical shift variation (-0.03 ppm) than H5' (-0.01 ppm). So it could be proposed that AMB got inserted from wide side of βCD cavity. Moreover, the upfield shifts of H3' and H5' protons signify the masking in presence of dense electronic clouds which results in shielding of protons. But in case of protons which are present outside the cavity such as H1', H4' H2' the variation of chemical shifts are little or none.

In Table 4b, the inclusion mode of the AMB+βCD can be further investigated by comparing the 1H NMR spectrum of Ambroxol in the absence and in presence of βCD. As showed in Fig. S10, mostly AMB signals appeared at 1.23-7.70 ppm, which was almost in similar with the βCD protons (2.13-4.98 ppm).Therefore, few AMB protons signals were overlapped specially around (3.4-5.0 ppm) region in the spectra of AMB+βCD complex. It was observed that AMB protons signals were much weaker as compared to βCD due to the less percentage of AMB (Guest) in the inclusion complex with βCD. Moreover, after inclusion in βCD chemical shift changes were also reported for AMB protons signals between free and complexed state (Table 4b). we observed that βCD induced variations in chemical shift occurred in case of few protons but pretty much significant differences as compared to αCD were reported in case of H4, H6 protons (Δδ: H4 -0.03; H6 -0.01), which were characterized by aromatic protons of benzene ring (Fig. S10). However, H12, H14 proton of AMB shows significant variations (Δδ: H12, H14 -0.03). From these findings it can also be proposed that probably the Aromatic ring of Ambroxol.HCl get stabilize outside the βCD cavity.

3.6. 2D-ROESY NMR spectral analysis.

Two-dimensional (2D) NMR spectroscopy provides significant information and conclusive evidence about the spatial proximity between the atoms of host and guest via observations of the intermolecular dipolar cross-correlations [35]. The two protons that are closely located in space within 0.4 nm can produce a nuclear Overhauser effect (NOE) cross-correlation in rotating-frame NOE spectroscopy (ROESY). Here we obtained 2D ROESY spectra of the inclusion complexes of AMB with αCD and βCD to procure more conformational information and encapsulation mechanism. The 2D-ROESY spectrum of the AMB+αCD complex (Fig. S11) showed considerable correlation of the aromatic H-6 and alicyclic H-11/H-15 protons of AMB with the H-5 and H-3 protons of αCD respectively. These results recommends that the AMB molecule was encapsulated within the cavity of αCD via the narrower rim, suggesting half of the aromatic ring containing bulky Br atoms outside the narrower rim and half of the alicyclic ring containing –OH group outside the wider

rim. The ROESY spectrum of the AMB+βCD complex (Fig. S12) also showed significant correlations between the aromatic H-6 and alicyclic H-12/H-14 protons of AMB with the H-3 and H-5 protons of βCD respectively. These outcomes, however, suggest that the AMB molecule was included in the βCD cavity via the wider rim, indicating half of the aromatic ring containing bulky Br atoms outside the wider rim. Based on the observation from ^{1}H-NMR and 2D-NMR, a plausible mechanism have been drawn and shown in scheme 2.

3.7. ESI-MS of the inclusion complex analysis:

The formation of the inclusion complexes of AMB with αCD and βCD were examined by ESI-mass spectrometry [36]. The spectra are shown in the Fig. S13 & S14 and the m/z values for the observed peaks are enlisted in Table 5. The peaks appeared at m/z 1388.58 and 1410.36 corresponds to the $[AMB+\alpha CD+H]^{+}$ and $[AMB+\alpha CD+Na]^{+}$ respectively, and the peaks at 1550.65 and 1572.44 corresponds to the $[AMB+\beta CD+H]^{+}$ and $[AMB+\beta CD+Na]^{+}$ respectively. These observed peaks in the spectra recommends that AMB is encapsulated inside the cyclodextrin cavity, and the stoichiometric ratio of the host-guest is 1:1.

3.8. Scanning Electron Microscope (SEM) analysis.

Scanning electron microscopy (SEM) is a very suitable qualitative analysis technique to visualize the surface texture of different materials [37]. SEM photographs of αCD, βCD, AMB and their inclusion complexes are shown in Fig. 6. Pure AMB shows its amorphous characteristics. The micrographs of βCD presented homogeneous morphology and polyhedral flake like crystals whereas αCD shows its well defined prismatic shape as reported in other literatures [38]. In contrast, the inclusion complex appeared as regular particles in which the original morphology of both components disappeared in both cases and homogeneous plate-like structures with crystal particles were present and it is quite different from the sizes and shapes of αCD, βCD and AMB, which confirms the formation of the inclusion complex.

3.9. Molecular Docking Results.

3.9.1 Prediction of AMB+αCD and AMB+βCD inclusion complexes binding mode.

Molecular modelling techniques, such as molecular docking, have been well recognised in predicting the binding modes [39] and interaction profiles of inclusion complexes with different receptor like structures including CDs [40]. Previous studies [41] have confirmed that the most of the guest molecules are usually inserted into CDs via the larger outer rim than that of the smaller one. But in our case, AMB+αCD showed different results (Fig. 7a & 7b) i.e, AMB has been inserted through narrow rim and aromatic ring was present almost outside, whereas cyclohexane ring was present at wider side of the ring. However, aromatic N-H were connected with CH_2-OH group of αCD through bond which make whole complex stabilized and the distance between these two group was found to be 2.13 Å (Table 6). The snapshots of AMB+βCD complexes illustrated in Fig. 7c & 7d show that AMB enters the nanocavity of the host in such a way that the both the bromine atoms of aromatic part was present outside of the wider rim of the cavity but benzyl carbon i.e, carbon next to the phenyl group attached with secondary group (-NH_2-) and whole cyclohexane ring were inserted into the cavity and stabilized at the norrower rim. The distance of secondary N-H group of AMB with the oxygen atom that attached with two glucopyranose rings of βCD was 2.36 Å, which connected by hydrogen bond (Table 6). In most of the previous studies show[42] that if both aromatic part and aliphatic part are present in a molecule, then most of the cases aromatic part got inserted but here, anomalous behaviour happen that may be due to the present of two bulky bromine atoms that present in the aromatic ring.

Moreover, the binding energy (ΔG^0) for the best docking pose of the complexes was also calculated at room temperature (Table 7). The ΔG^0 values of modes AMB+αCD and AMB+βCD in the 1:1 stoichiometry were -3.68 and -4.57 kcal/mol, respectively obtained from the S dock score of MOE database viewer. The results indicated that the complex were stable by good binding energy and drug were completely embedded into the CD cavities and the computational data is quite

comparable with our experimental data which is in the range of -4.86 kcal/mol to -6.01 kcal/mol and -5.96 to -6.91 kcal/mol for AMB+αCD and AMB+βCD inclusion complex respectively (Table 2). The findings of this theoretical study are consistent with the results of UV-vis titration, FT-IR, NMR and ESI-MS study.

3.9.2. Potential energy calculations of two different inclusion complexes (AMB+αCD and AMB+βCD).

Changes in Potential energy (ΔE) for both the complexes were also calculated in order to obtain some profound information about the geometry of the host–guest complexes and to find the intermolecular interaction in between host and guest inclusion complexation [43]. ΔE of the complexation was calculated for the minimum energy mode of docked complex according to Eq. (1) and the data of $E_{complex}$, E_{host} + E_{guest}, ΔE were listed in Table 8. Solvation energy is zero because the modeling was carried out in gas phase.

$$\Delta E = E_{Complex}-(E_{Host}+E_{Guest}) \ldots\ldots\ldots (1)$$

The results show that the potential energies for the complexes of AMB with αCD and βCD were -174.886 kcal mol^{-1} and -213.260 kcal mol^{-1}, respectively, indicating that AMB has stronger affinity for βCD than that for Acd [44]. Electrostatic potential energy surfaces of both the complex show the charge distribution of molecule three dimensionally (Fig. 8). Sherje et al., [45] in their work, beautifully showed that various potential energy components have overall effect on forming stable inclusion complex. In our case of AMB+αCD inclusion complex (Table S8), Van der walls energy (vdw) was found to be 170.84 kcal/mol and electrostatic interaction energy (ele) was about 172.20 kcal/mol. So, the differential (Del) van der Waals energy was 44.88 kcal/mol, and the Del electrostatic energy was −12.51 kcal/mol. It is the van der Waals energy that makes the inclusion complex stable. However, in case of AMB+βCD inclusion complex (Table S9), Van der walls energy (vdw) was found to be 175.33 kcal/mol and electrostatic interaction energy (ele) was about 268.75 kcal/mol. So, the differential (Del) van der Waals energy was 9.45

kcal/mol, and the Del electrostatic energy was 42.85 kcal/mol. It is the electrostatic interaction energy that makes the inclusion complex stable [46,47].

3.9.3. Change in the dihedral angle and bond length of AMB after forming inclusion complexes.

To establish the modification of the structural conformation of AMB upon insertion into αCD and βCD, we have once used MD docking. Sancho et al., [48] showed that change in dihedral angle and bond length could give us strong evidence of conformational changes. After getting the docked pose of all the inclusion complexes, we have measured the dihedral angle of free AMB and the complex encapsulated AMB. The calculated dihedral angles of pure AMB between the carbon atoms labeled as a-b-c-d, b-c-d-e and b-c-d-f were found to be 172.1^0, 66.4^0, and -168.5^0 respectively (Scheme 1). However, for inclusion complex AMB+αCD, the dihedral angles for the same labelling were found to be -174.9^0, -70.9^0 and 172.7^0. It is clear evidence that all the planes were rotated to their opposite direction after forming complex. But in case of AMB+βCD complex, the dihedral angles were found to be 81.8^0, 152.6^0 and -86.8^0. It suggests that all the planes were getting shifted to get the stability of the complex. Docking poses all supports the conclusion as in encapsulated form, AMB got deformed structure. Change in bond length of guest AMB also confirms structural changes in both the inclusion complexes. In free AMB, Bond length of aromatic amine **N-H** bond is around 0.86Å. Whereas, aliphatic $\mathbf{N_c}$-$\mathbf{C}H_2$, Ph-$\mathbf{C_b}$-**H** is about 1.45Å and 0.97Å respectively. When it forms inclusion complex, aromatic amine **N-H** bond slightly shifted from 0.86Å to 1.03Å in case of AMB+αCD due to hydrogen bonding with hydroxyl group of αCD and 0.86Å to 1.01Å in case of AMB+βCD due to van der Waals force of attraction. While, aliphatic $\mathbf{N_c}$-$\mathbf{C}H_2$ gets increased from 1.45Å to 1.47Å in AMB+αCD and 1.50Å in case of AMB+βCD. In addition, Ph-$\mathbf{C_b}$-**H** bond length is also increased from 0.97Å to 1.08Å in case of AMB+αCD and 1.10Å in case of AMB+βCD respectively possibly due to the hydrophobic interaction of inner cavity protons.

3.9.4 Molecular dynamics (MD) simulations.

Molecular dynamics and simulations (MD/MS) study was performed on both of the inclusion complexes to check the stability of the host-guest complex with respect to time [49,50]. Optimized Inclusion complexes obtained after docking were simulated in gas phase from 0 picoseconds to 600 picoseconds (100ps of equilibrium and 500ps of production) with respect to temperature, potential energy and kinetic energy. Before simulation process, whole complex systems were energy minimized. Simulation study of AMB+αCD inclusion complex revealed that initially potential energy of the complex was found to be 283.90 kcal/mol, with the increase in time energy get decreasing and a mild break point found after 150ps the whole assemble get stabilized after 150ps and it stayed stabilised up to 600ps with 333.81 kcal/mol energy respect to temperature, potential energy and kinetic energy, as shown in Figure 9(a–c), respectively [51,52]. In case of AMB+βCD complex, initial potential energy was found to be 349.53 kcal/mol. At around 120ps, potential energy was 454.85 kcal/mol, then, a sharp break in the curve was observed and potential energy drop down to 432.29 kcal/mol and with increase in time potential energy getting decrease and stabilized upto 371.30 kcal/mol at 600ps Figure 10(a–c).

4. CONCLUSIONS:

In this paper, we report structural and conformational changes after inclusion of AMB with two different host molecules. The thermodynamic data for two inclusion complexes (AMB+αCD and AMB+βCD) make us understand that AMB has been encapsulated with ease. Despite the structural similarity between these two hosts, their inclusion complexes show interesting differences with respect to their dihedral angle changes and potential energy changes. Inclusion mechanism has been outlined from various spectroscopic methods, e.g, Job's plot, ^{1}H-NMR, 2D-NMR, ESI-MS. Then, it is finally confirmed by molecular docking method and theoretically predicts their binding modes. Potential energy calculation indicates that after inclusion complexation of AMB in β-cyclodextrin give more stabilization than that of

in α-cyclodextrin. Molecular docking poses of both the complexes confirm that conformational changes occur after encapsulation. Dynamic simulation also confirms that β-CD-complex after a certain time gives more stabilization than α-CD-complex and their dynamic behaviour with respect to time (ps).

Supporting Information:

Detailed descriptions of all the chemicals used, job plots, association constants data, van't Hoff plot of $\ln K_a$ vs 1/T, 2D-NMR and ESI-MS spectra of inclusion complexes are given. Potential energy calculations of both inclusion complexes by computational studies are shown. Three dimensional linkage of inclusion complex with protein has been obtained.

Acknowledgement:

This work was supported by State fellowship (Ref No. 600/R-2018) to NR given by Govt of west Bengal. Co-author PB is very grateful to UGC for getting Junior Research fellowship (Ref No. 222/(CSIR-UGC NET DEC. 2017)). Corresponding author Prof. M. N. Roy is very much thankful to UGC for getting one time Grant of seven lakh from UGC-BSR (Ref. No. F.4-10/2010).

Conflict of interest

The author declare no conflict of interest

TABLES

System	Temperature (K)	Slope	Intercept	Association constant (Ka)/(M^{-1})
AMB+αCD	293.15	0.000725	3.06391	4226±1195
	303.15	0.000456	4.10125	8993±1765
	313.15	0.000447	7.08252	15799±172
AMB+βCD	293.15	0.000283	7.86202	27780±2570
	303.15	0.000242	9.03459	37333±1036
	313.15	0.000239	10.84575	45379±821

Table 1: Association constant of the Inclusion complex between AMB, αCD & βCD at three different Temperatures; ± sign indicates the standard deviation

System	Temp(K)	Ka/M^{-1}	ΔH^0/KJ mol^{-1}	ΔS^0/KJ mol^{-1} K^{-1}	ΔG KJ mol^{-1}	ΔG KCal mol^{-1}
AMB+αCD	293.15	4226	50.3166	0.2411	-20.3649	-4.86
	303.15	8993			-22.7760	-5.44
	313.15	15799			-25.1871	-6.01
AMB+βCD	293.15	27780	18.7543	0.1490	-24.9483	-5.96
	303.15	37333			-26.4391	-6.31
	313.15	45379			-28.9299	-6.91

Table 2: Various thermodynamic parameters of AMB+αCD and AMB+βCD complex system (1 cal= 4.184 J)

Protons Of αCD	Δδ (Free) (ppm)	Δδ (Complex) (ppm)	Δδ (Difference) (ppm)
H1'	4.97-4.96 (d, J=4Hz)	4.96 (d, J=4Hz)	-0.01
H4'	3.50-3.47 (t, J=12Hz)	3.50-3.47 (t, J=12Hz)	0.00
H3'	3.91-3.80 (dd, J=8Hz)	3.87-3.81 (t, J=8Hz)	**-0.04**
H5'	3.79-3.74 (m, J=8Hz)	3.79-3.75 (t, J=8Hz)	**-0.01**
H2'	3.56-3.52 (dd, J=4Hz)	3.56-3.52 (dd ,J=4Hz)	0.00

Table 3a: Chemical shift data (in ppm) of protons of free αCD and of AMB+αCD complex and their differences

PROTONS OF AMB	δ(Free) (ppm)	δ(Complex) (ppm)	δ(Difference) (ppm)
H4	7.70 (1H, s)	7.72 (1H, s)	0.02
H6	7.33 (1H, s)	7.36 (1H, s)	0.03
H8	2.00-1.97 (1H, d, J=12Hz)	2.01-1.97 (1H, d, J=12Hz)	0.01
H9	2.14-2.12 (1H, d, J=12Hz)	2.18-2.16 (1H, d, J=12Hz)	0.04
H10	3.18-3.12 (1H, t, J=12Hz)	-	0
H13	3.61-3.56 (1H, m, J=4Hz)	_	_
H12, H14	1.49-1.40 (4H, q, J=12Hz)	1.44 (4H, q, J=12Hz)	-0.05
H11, H15	1.32-1.23 (4H, q, J=12Hz)	1.30 (4H, q, J=12Hz)	-0.02
H16	4.15 (2H, s)	4.17 (1H, s)	0.02

Table 3b: Chemical shift Data (in ppm) of protons of AMB in Free State and during Inclusion Complexation with αCD

PROTONS OF βCD	δ(Free) (ppm)	δ(Complex) (ppm)	Δδ(Difference) (ppm)
H1'	4.98-4.97 (d, J=4Hz)	4.98-4.97 (d, J=4Hz)	0
H4'	3.49-3.47 (t, J=12Hz)	3.49-3.47 (t, J=12Hz)	0.00
H3'	3.90-3.86 (t, J=8Hz)	3.87-3.83 (t, J=8Hz)	**-0.03**
H5'	3.79-3.75 (t, J=8Hz)	3.78-3.75 (t, J=8Hz)	**-0.01**
H2'	3.57-3.54 (dd, J=4Hz)	3.57-3.51 (dd ,J=4Hz)	0.00

Table 4a: Chemical shift Data (in ppm) of protons of βCD in Free State and during Inclusion Complexation with AMB

PROTONS OF AMB	δ(Free) (ppm)	δ(Complex) (ppm)	δ(Difference) (ppm)
H4	7.70 (1H, s)	7.67 (1H, s)	**-0.03**
H6	7.33 (1H, s)	7.32 (1H, s)	**-0.01**
H8	2.00-1.97 (1H, d, J=12Hz)	2.03-1.99 (1H, d, J=12Hz)	0.03
H9	2.14-2.12 (1H, d, J=12Hz)	2.17-2.14 (1H, d, J=12Hz)	0.03
H10	3.18-3.12 (1H, t, J=12Hz)	-	0
H13	3.61-3.56 (1H, m, J=4Hz)	-	-
H12, H14	1.49-1.40 (4H, q, J=12Hz)	1.46-1.43 (4H, q, J=12Hz)	**-0.03**
H11, H15	1.32-1.23 (4H, q, J=12Hz)	1.32-1.25 (4H, q, J=12Hz)	0
H16	4.15 (2H, s)	4.15 (1H, s)	0

Table 4b: Chemical shift Data (in ppm) of protons of AMB in Free State and during Inclusion Complexation with βCD

Name of the complexes	Calculated mass (a.u)	Experimental mass (a.u)
$[AMB+\alpha CD+H]^+$	1388.41	1388.58
$[AMB+\alpha CD+Na]^+$	1410.41	1410.36
$[AMB+\beta CD+H]^+$	1550.53	1550.65
$[AMB+\beta CD+Na]^+$	1572.53	1572.44

Table 5: ESI-MS mass spectra of different inclusion complex.

Receptor atoms	AMB atoms	Distance (Å)
αCD (CH_2-O)	**N**(aromatic)**-H**	2.13
βCD (pyranoseCH_2-O-CH_2pyranose)	**N**(SP^3)**-H**	2.36

Table 6: Hydrogen bonding distance in AMB+αCD and AMB+βCD Complex from Molecular Docking

Ligand with receptor	Binding affinity(ΔG) in kcal.mol^{-1}	rmsd_refine
AMB+αCD	-3.68	3.95
AMB+βCD	-4.57	2.31

Table 7: Binding affinity of AMB+αCD and AMB+βCD obtained from Molecular Docking

Inclusion Complex	E_{Host} (Kcal/mol)	E_{Guest} (Kcal/mol)	$E_{Complex}$ (Kcal/mol)	ΔE (Kcal/mol)
AMB+αCD	511.134	254.702	590.950	-174.886
AMB+βCD	1253.700	254.702	1295.142	-213.260

Table 8: potential energy calculation of the docked complex without energy minimization

Compound name	Molecular formula	Molecular weight	CAS number	Purity	Purchased from
Ambroxol Hydrochloride	$C_{13}H_{18}Br_2N_2O.HCl$	414.57	23828-92-4	>98.0%	From TCI Chemicals (India) Pvt. Ltd
αCD	$C_{36}H_{60}O_{30}$	972.84	10016-20-3	>97.0%	SIGMA- ALDRICH India
βCD	$C_{42}H_{70}O_{35}$	1134.98	7585-39-9	>98.0%	SIGMA- ALDRICH India

Table S1: Description of the Materials purchased for the Study

AMB (ml)	αCD (ml)	AMB (μM)	αCD (μM)	[AMB] /([AMB]+[αCD])	Absorbance(A)	ΔA	ΔA*[AMB] /([AMB]+[αCD])
4	0	100	0	1	0.944749069	0	0
3.6	0.4	90	10	0.9	0.886510836	0.058238233	0.05241441
3.2	0.8	80	20	0.8	0.789445711	0.155303358	0.124242686
2.8	1.2	70	30	0.7	0.683141762	0.261607307	0.183125115
2.4	1.6	60	40	0.6	0.589171968	0.355577101	0.213346261
2	2	50	50	0.5	0.470462244	0.474286825	0.237143412
1.6	2.4	40	60	0.4	0.426916412	0.517832658	0.207133063
1.2	2.8	30	70	0.3	0.371819527	0.572929542	0.171878863
0.8	3.2	20	80	0.2	0.297813262	0.646935807	0.129387161
0.4	3.6	10	90	0.1	0.255634679	0.689114390	0.068911439
0	4	0	100	0	0.000000000	0.944749069	0

Table S2: Datasheet for plotting Job's Plot in case of AMB+αCD system

AMB (ml)	βCD (ml)	AMB (μM)	βCD (μM)	[AMB]/ ([AMB]+[βCD])	Absorbance(A)	ΔA	ΔA*[AMB]/([AMB]+[βCD])
4	0	100	0	1	1.044322491	0000000000	0000000000
3.6	0.4	90	10	0.9	0.856930733	0.187391758	0.168652582
3.2	0.8	80	20	0.8	0.768405914	0.275916576	0.220733261
2.8	1.2	70	30	0.7	0.686136742	0.358185749	0.250730024
2.4	1.6	60	40	0.6	0.587579975	0.456742516	0.274045509
2	2	50	50	0.5	0.490162849	0.554159641	0.277079821
1.6	2.4	40	60	0.4	0.446716309	0.597606182	0.239042473
1.2	2.8	30	70	0.3	0.321279526	0.723042965	0.216912889
0.8	3.2	20	80	0.2	0.306833267	0.737489223	0.147497845
0.4	3.6	10	90	0.1	0.298838615	0.745483875	0.074548388
0	4	0	100	0	0.000000000	1.044322491	0000000000

Table S3: Datasheet for plotting Job's Plot in case of AMB+βCD system

temp/k	[AMB] /μM	[αCD] /μM	A_o	A	ΔA	1/[αCD]/M^{-1}	1/ΔA	Intercept	Slope	Ka/M^{-1}
	50	10	0.37445	0.38771	0.01326	100000	75.41478			
	50	20	0.37445	0.39509	0.02064	50000	48.44961			
293.15	50	30	0.37445	0.41353	0.03908	33333	25.58854	3.06391	0.000725	4226
	50	40	0.37445	0.42117	0.04672	25000	21.40411			
	50	50	0.37445	0.43218	0.05773	20000	17.32202			
	50	10	0.3682	0.38848	0.02028	100000	49.30966			
	50	20	0.3682	0.40114	0.03294	50000	30.35823			
303.15	50	30	0.3682	0.41172	0.04352	33333	22.97794	4.10125	0.000456	8993
	50	40	0.3682	0.43314	0.06494	25000	15.39883			
	50	50	0.3682	0.46980	0.10160	20000	9.84252			
	50	10	0.39789	0.41724	0.01935	100000	51.67959			
	50	20	0.39789	0.43045	0.03256	50000	30.71253			
313.15	50	30	0.39789	0.44132	0.04343	33333	23.02556	7.06252	0.000447	15799
	50	40	0.39789	0.45261	0.05472	25000	18.27485			
	50	50	0.39789	0.46710	0.06921	20000	14.44878			

Table S4: Changes in the absorption intensity of the AMB at different temperature as a function of the αCD's concentration.

Temp (K)	Ka /M^{-1}	1/T	lnKa	intercept	slope	ΔH^0 /J mol^{-1}	ΔS^0 /J mol^{-1} K^{-1}	$\Delta G^0 = (\Delta H^0 - T\Delta S^0)$ $Jmol^{-1}$	ΔG KJ mol^{-1}
293.15	4226	0.00341	18.34901					-20364.9319	-20.3649
303.15	8993	0.00329	89.10420	28.99881	-6051.67364	50316.6405	241.1106	-22776.0379	-22.7760
313.15	15799	0.00319	39.66770					-25187.1439	-25.1871

Table S5: Thermodynamic parameters calculated from Van't Hoff equation for AMB+αCD system.

Temp /k	[AMB] /Mm	[βCD] /μM	$A_\circ$	A	ΔA	1/[βCD] /M^{-1}	1/ΔA	Intercept	Slope	Ka /M^{-1}
	50	10	0.473750948	0.501577377	0.027826430	100000	35.93706			
	50	20	0.473750948	0.514558563	0.040807615	50000	24.50523			
293.15	50	30	0.473750948	0.525943719	0.052192771	33333	19.15974	7.86202	0.000283	27780
	50	40	0.473750948	0.544928169	0.071177221	25000	14.04944			
	50	50	0.473750948	0.553185902	0.079434954	20000	12.58892			
	50	10	0.498450277	0.528552834	0.030102557	100000	33.21977			
	50	20	0.498450277	0.543729450	0.045279173	50000	22.08521			
303.15	50	30	0.498450277	0.558877945	0.060427668	33333	16.54871	9.03459	0.000242	37333
	50	40	0.498450277	0.563250542	0.064800265	25000	15.43204			
	50	50	0.498450277	0.571950893	0.073500616	20000	13.60533			
	50	10	0.503956196	0.533198120	0.029241924	100000	34.19748			
	50	20	0.503956196	0.540121608	0.036165411	50000	27.65073			
313.15	50	30	0.503956196	0.548247859	0.044291663	33333	22.57761	10.84575	0.000239	45379
	50	40	0.503956196	0.563841820	0.059885623	25000	16.69850			
	50	50	0.503956196	0.589945619	0.085989423	20000	11.62934			

Table S6: Changes in the absorption intensity of the AMB at different temperature as a function of the βCD concentration

Temp (K)	Ka/M^{-1}	1/T	lnKa	intercept	slope	ΔH^0 /J mol^{-1}	ΔS^0 /J mol^{-1} K^{-1}	$\Delta G^0 = (\Delta H^0 - T\Delta S^0)$ $Jmol^{-1}$	ΔG KJ mol^{-1}
293.15	27780	0.003411	10.23207					-24948.3955	-24.9483
303.15	37333	0.003298	10.52763	17.93009	-2255.61593	18754.3186	149.0797	-26439.1925	-26.4391
313.15	45379	0.003193	10.72280					-27929.9895	-28.9299

Table S7: Thermodynamic parameters calculated from Van't Hoff equation for AMB+βCD system.

Name	Bond stretching (Str)	Bond angle (angle)	Stretching-bend interaction (Stb)	Out of plane bending (oop)	Dihedral torsional (tor)	Van der walls energy (vdw)	Electrostatic interaction (ele)	Solvation energy (sol)	Total energy (E)
AMB	148.338	7.168	0.154	32.437	6.571	56.240	3.793	00	254.702
αCD	16.578	60.293	-0.392	00	123.987	125.953	184.715	00	511.134
AMB+αCD IC	20.801	67.653	-0.298	28.285	131.465	170.842	172.203	00	590.950

Table S8: Potential energy of AMB, αCD and AMB+αCD inclusion complex and its various components

Name	Bond stretching (Str)	Bond angle (angle)	Stretching-bend interaction (Stb)	Out of plane bending (oop)	Dihedral torsional (tor)	Van der walls energy (vdw)	Electrostatic interaction (ele)	Solvation energy (sol)	Total energy (E) (Kcal/mol)
AMB	148.338	7.168	0.154	32.437	6.571	56.240	3.793	00	254.702
βCD	610.025	89.632	-2.827	00	135.077	165.889	225.909	00	1253.700
AMB+βCD IC	613.378	98.799	-2.602	0.014	141.468	175.333	268.751	00	1295.142

Table S9: Potential energy of AMB, βCD and AMB+βCD inclusion complex and its various components

FIGURES

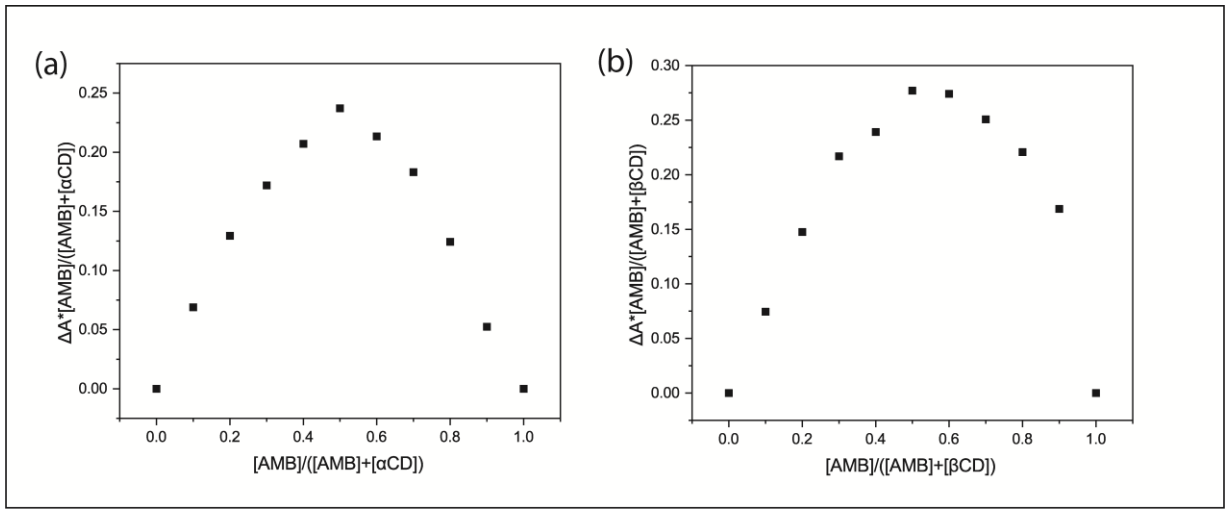

Fig. 1: Job's Plot of the (a) AMB+αCD and (b) AMB+βCD system at 298.15K

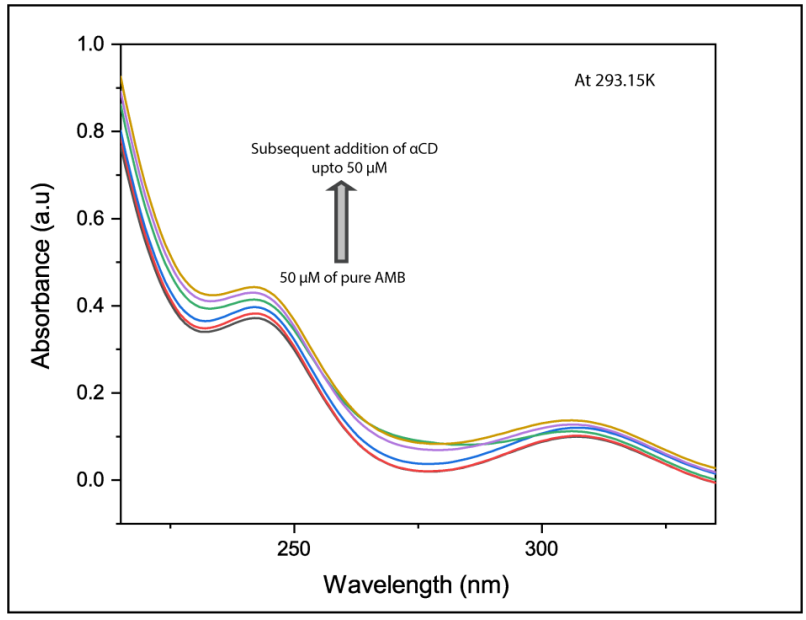

Fig. 2: Variation of UV-vis spectra in subsequent addition of αCD in 50μM aqueous solution of AMB at 293.15K

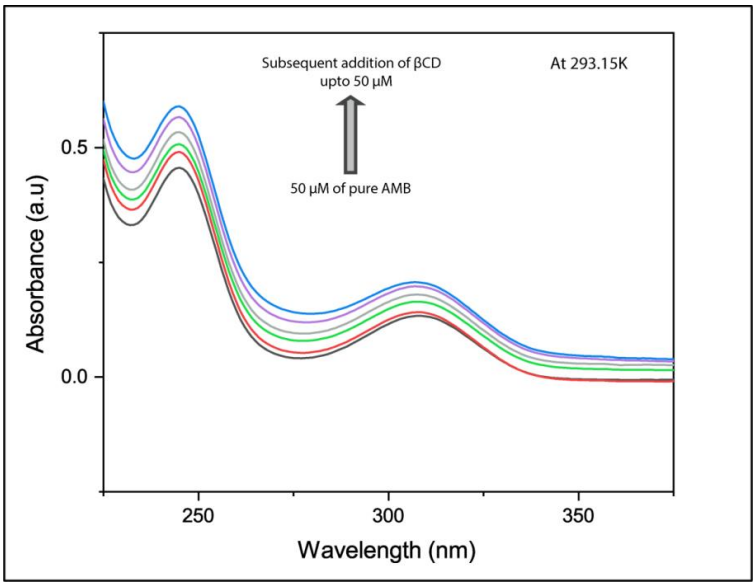

Fig. 3: Variation of UV-vis spectra in subsequent addition of βCD in 50μM aqueous solution of AMB at 293.15K

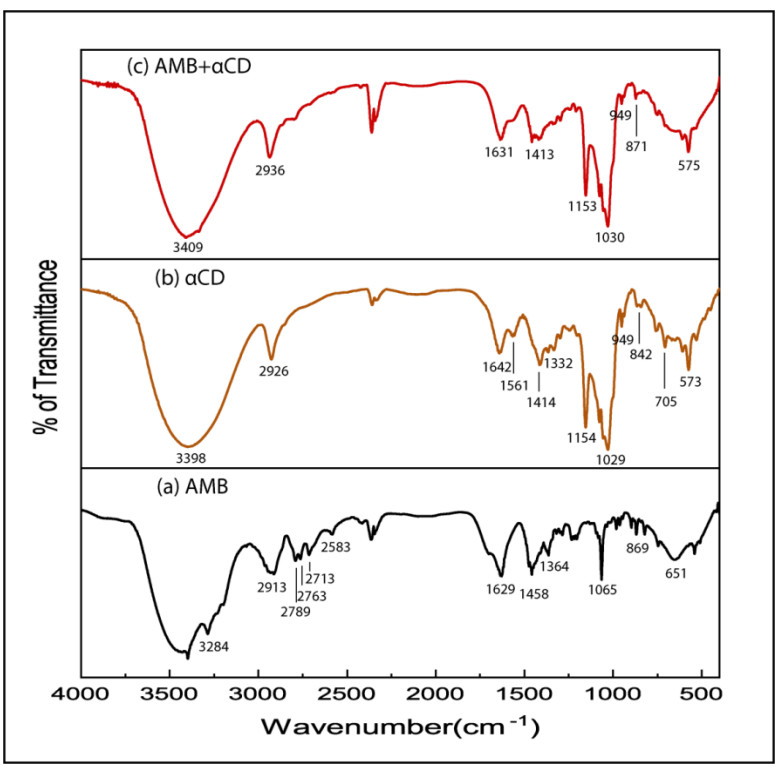

Fig. 4: FTIR spectra of (a) pure AMB (b) αCD (c) AMB+αCD inclusion complex

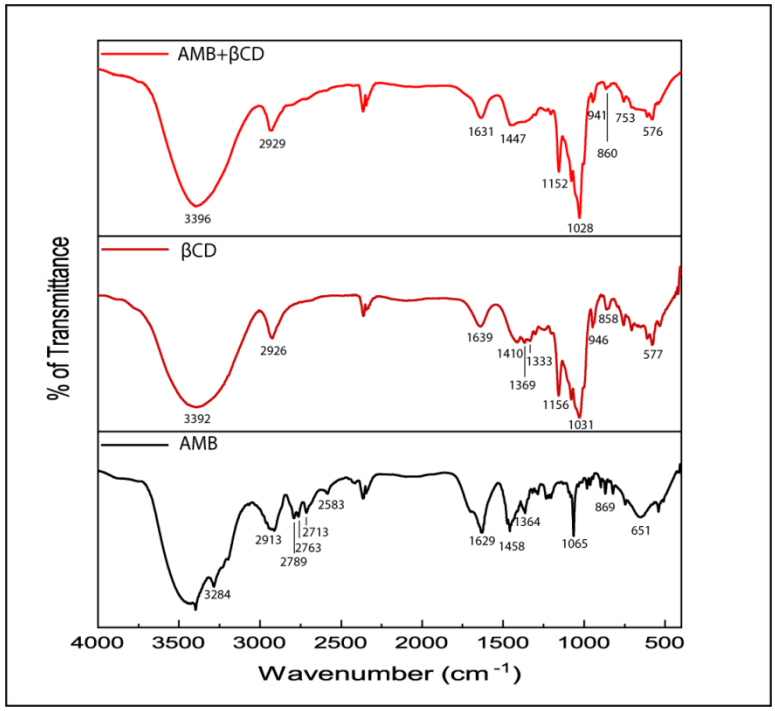

Fig. 5: FTIR spectra of (a) pure AMB (b) βCD (c) AMB+βCD inclusion complex

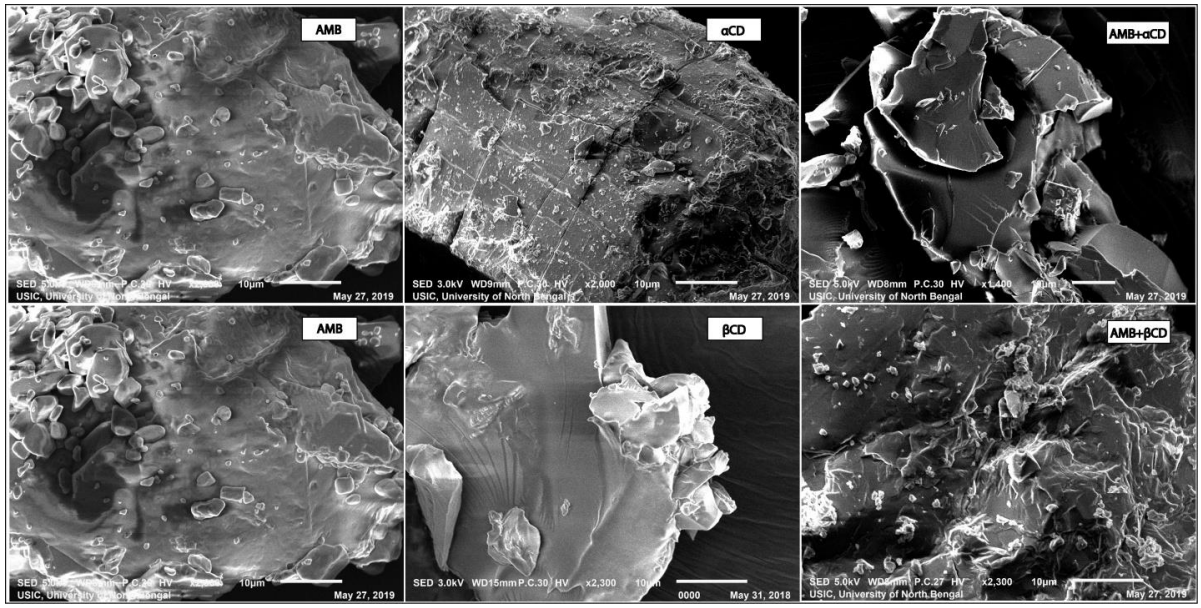

Fig. 6: Scanning Electron Microscope microphotograph of AMB, αCD, βCD, AMB+αCD complex and AMB+βCD complex

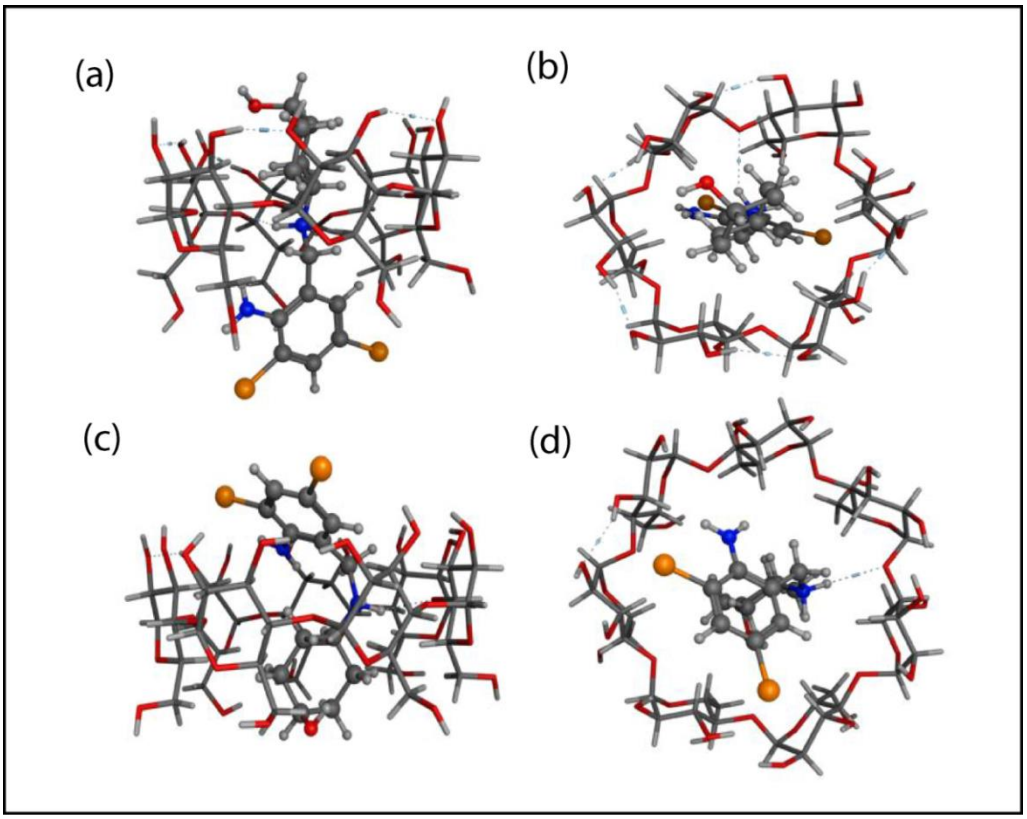

Fig. 7: (a) AMB+αCD Side view; (b) AMB+αCD Upper view; (c) AMB+βCD side view; (d) AMB+βCD Upper view; atom designation: gray, carbon; red, oxygen; blue, nitrogen; orange, bromine.

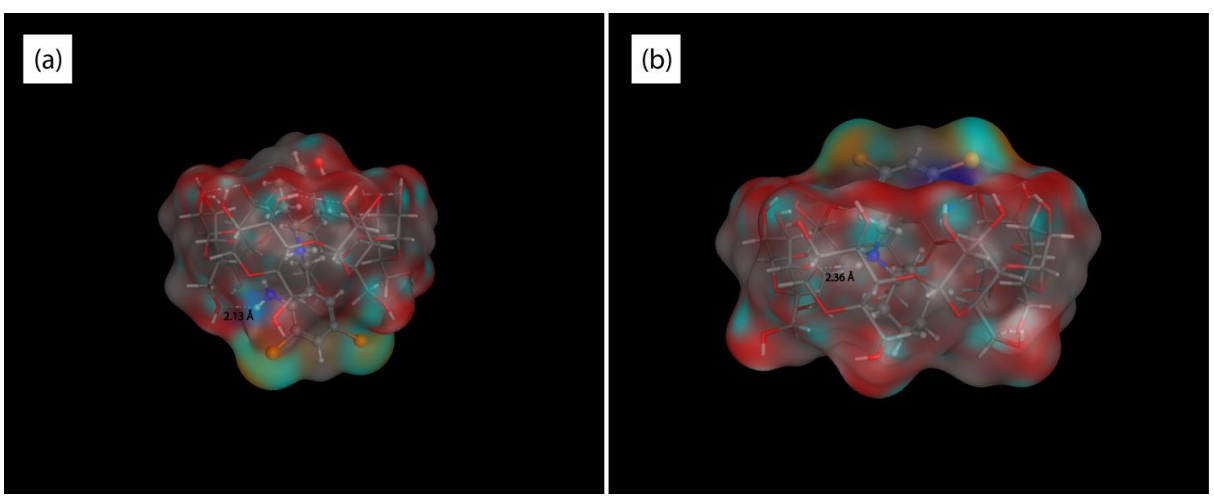

Fig. 8: electrostatic potential energy surface of (a) AMB+αCD (b) AMB+βCD inclusion complex

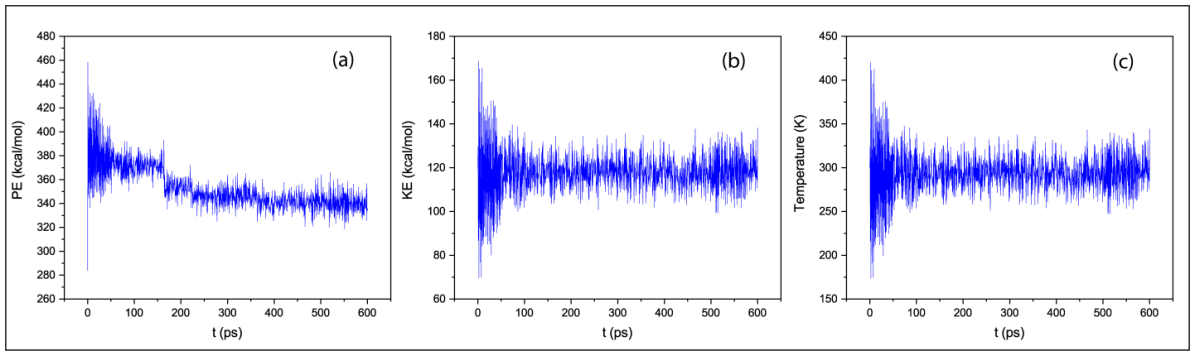

Fig 9: Molecular dynamic simulation study of AMB+αCD inclusion complex with respect to (a) time versus kinetic energy (b) time versus potential energy (c) time versus temperature.

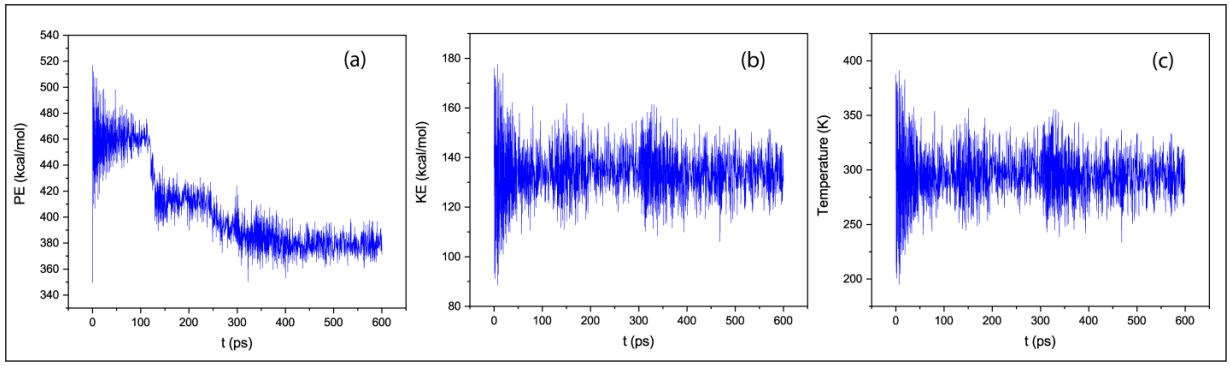

Fig 10: Molecular dynamic simulation study of AMB+βCD inclusion complex with respect to (a) time versus kinetic energy (b) time versus potential energy (c) time versus temperature.

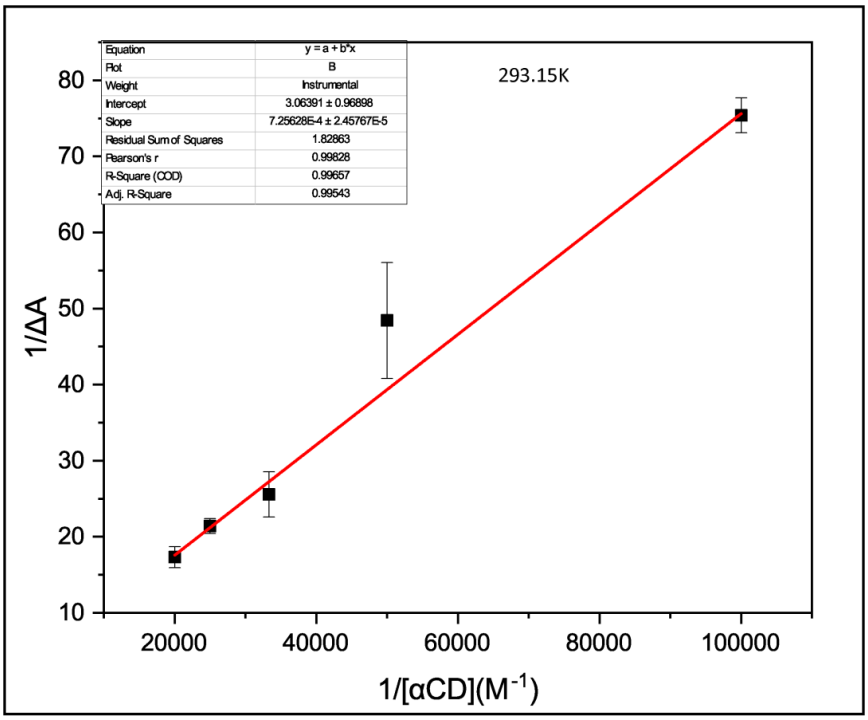

Figure S1: Double reciprocal plot using the Benesi–Hildebrand Method to obtain Slope and intercept of the straight line at 293.15K Temperature for AMB+αCD system

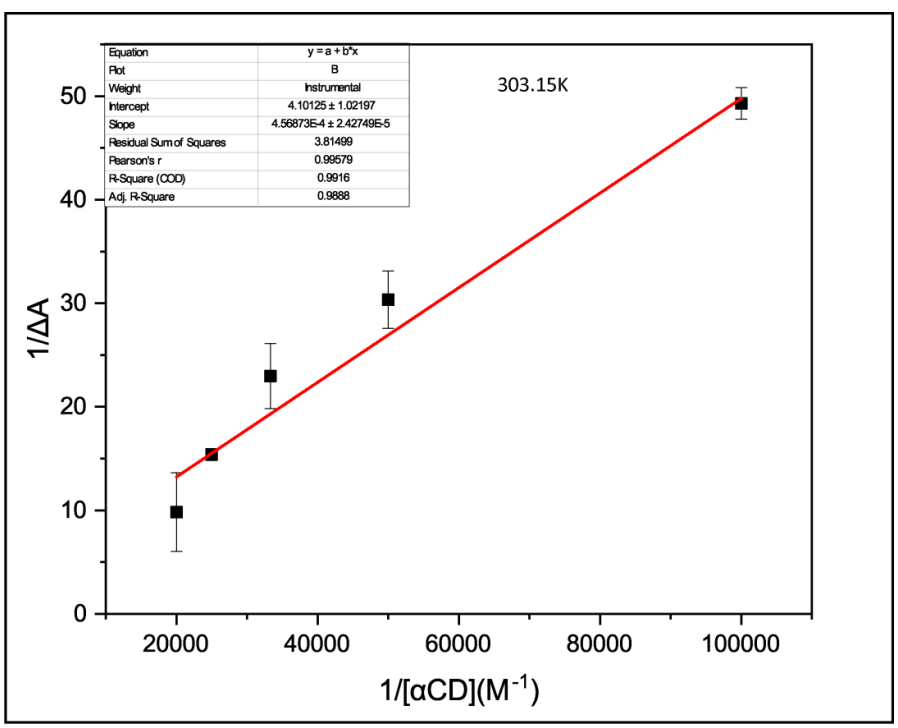

Figure S2: Double reciprocal plot using the Benesi–Hildebrand Method to obtain Slope and intercept of the straight line at 303.15K Temperature

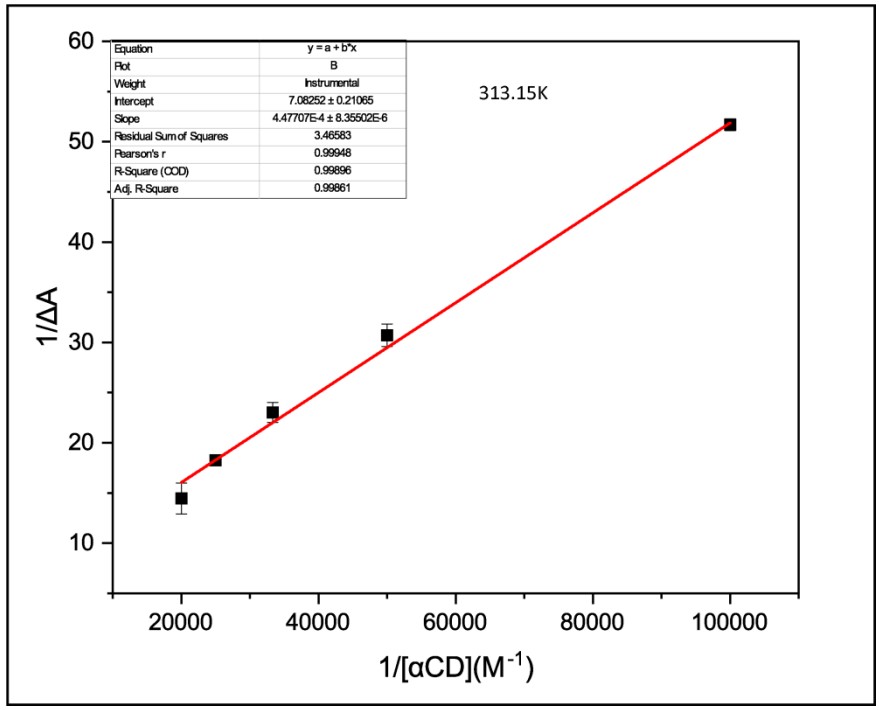

Figure S3: Double reciprocal plot using the Benesi–Hildebrand Method to obtained Slope and intercept of the straight line at 313.15K Temperature

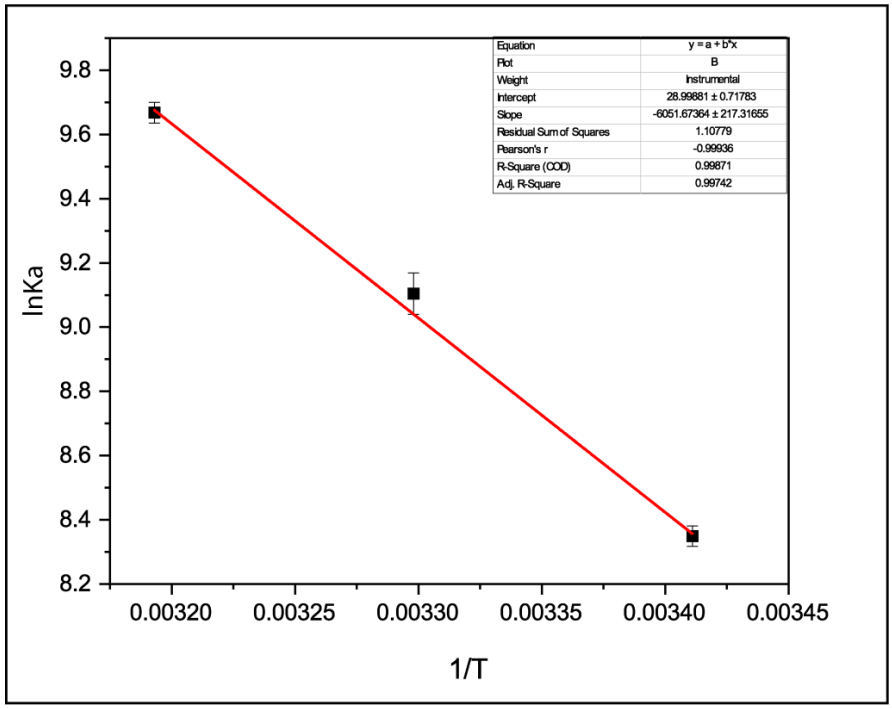

Figure S4: Plot of $\ln K_a$ vs 1/T for the interaction of AMB with αCD

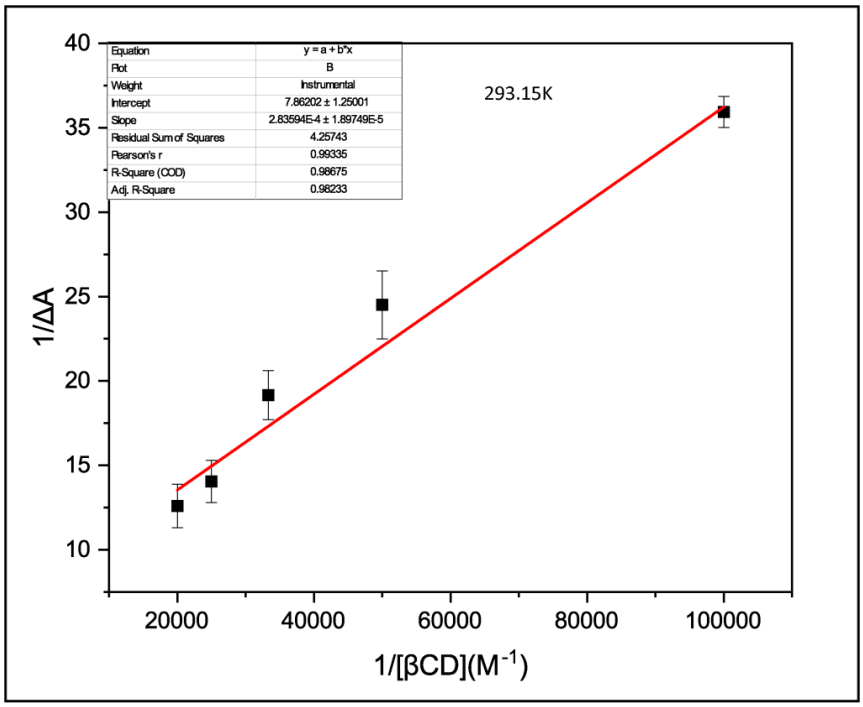

Figure S5: Double reciprocal plot using the Benesi–Hildebrand Method to obtained Slope and intercept of the straight line at 293.15K Temperature

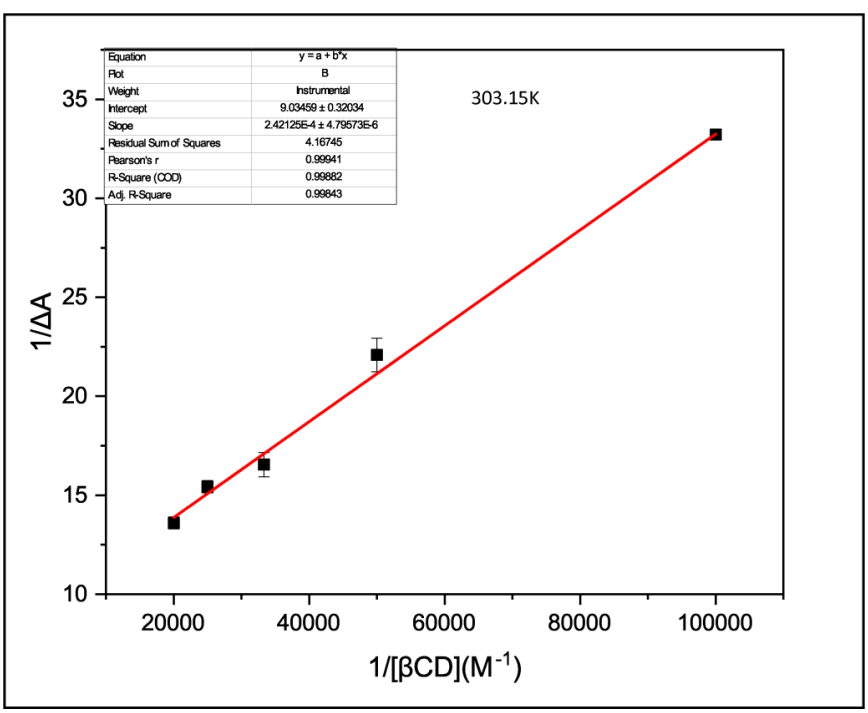

Figure S6: Double reciprocal plot using the Benesi–Hildebrand Method to find out the Slope and intercept of the straight line obtained at 303.15K Temperature

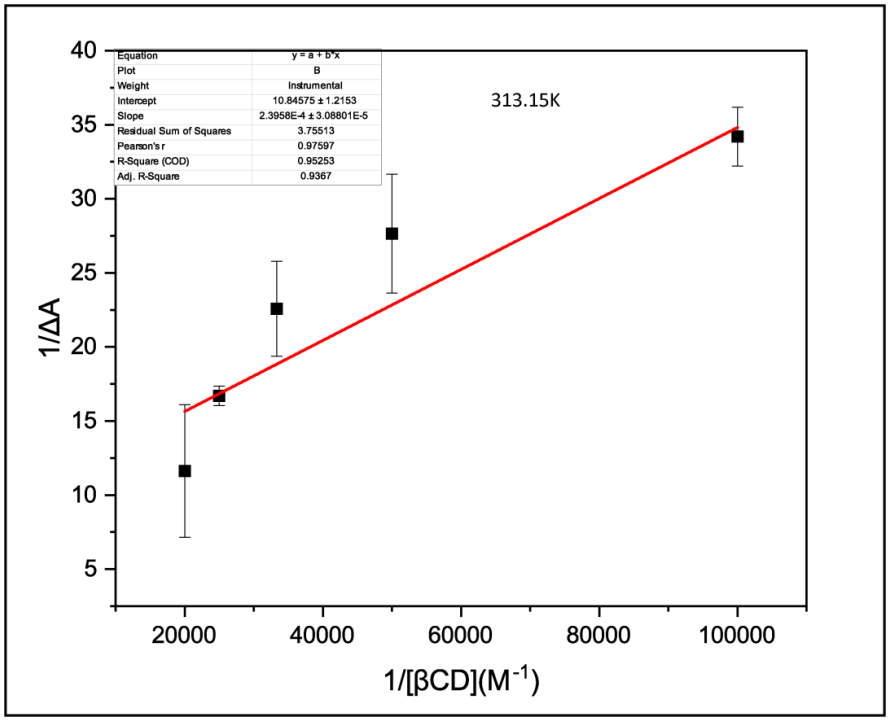

Figure S7: Double reciprocal plot using the Benesi–Hildebrand Method to find out the Slope and intercept of the straight line obtained at 313.15K Temperature

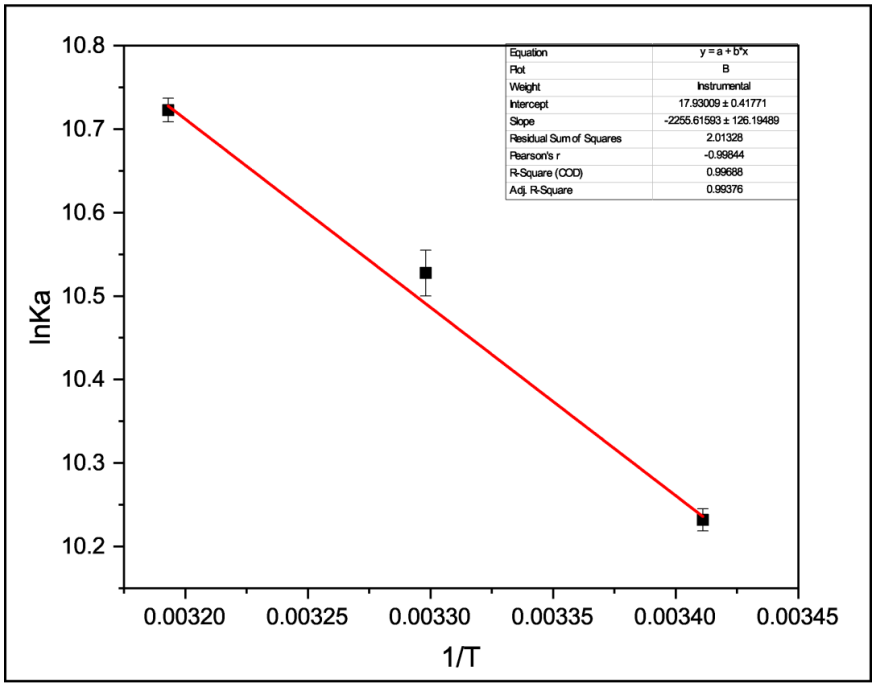

Figure S8: Plot of $\ln K_a$ vs 1/T for the interaction of AMB with βCD

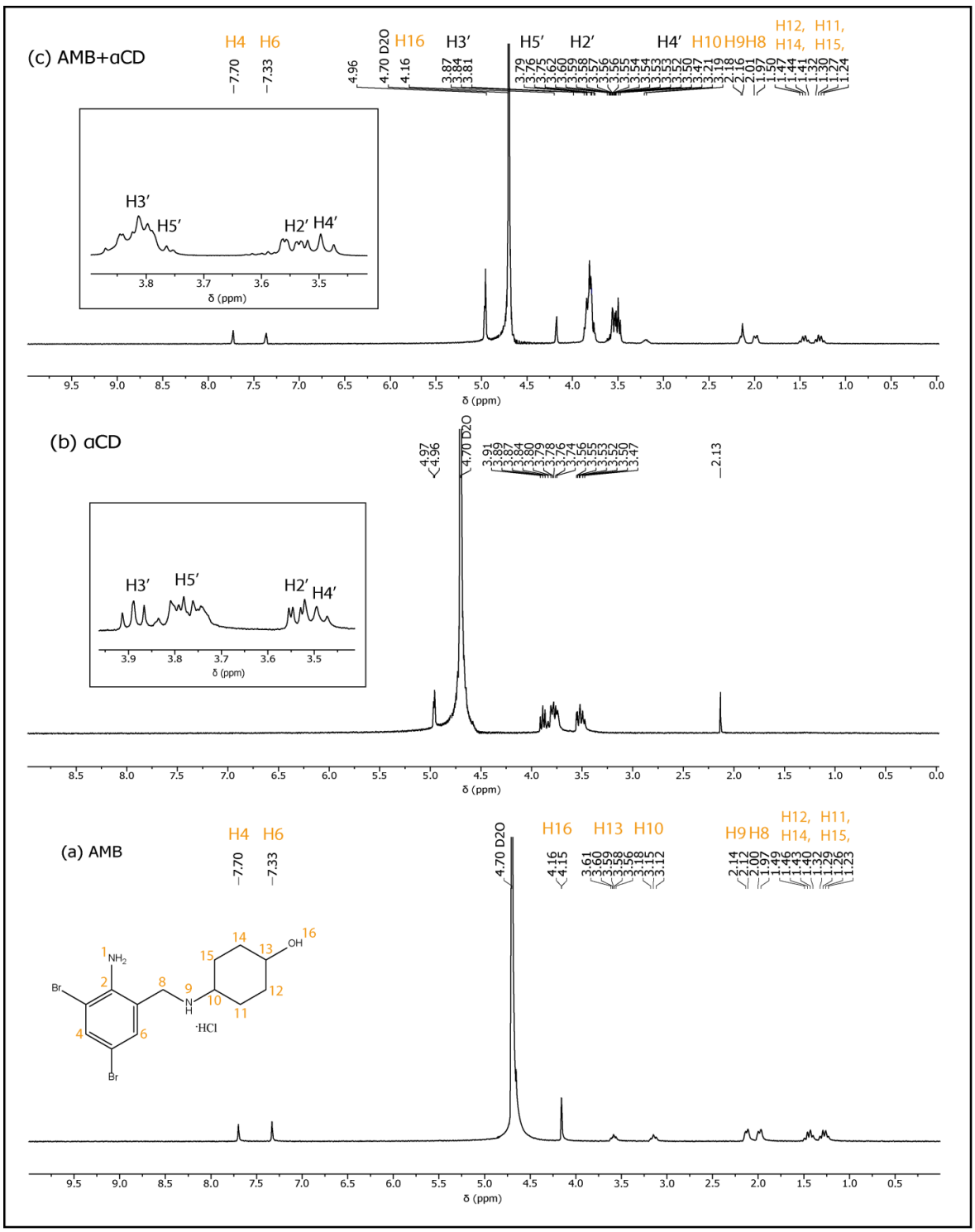

Fig. S9: ^{1}H-NMR spectra of (a) Free AMB (b) αCD (c) AMB+αCD inclusion complex

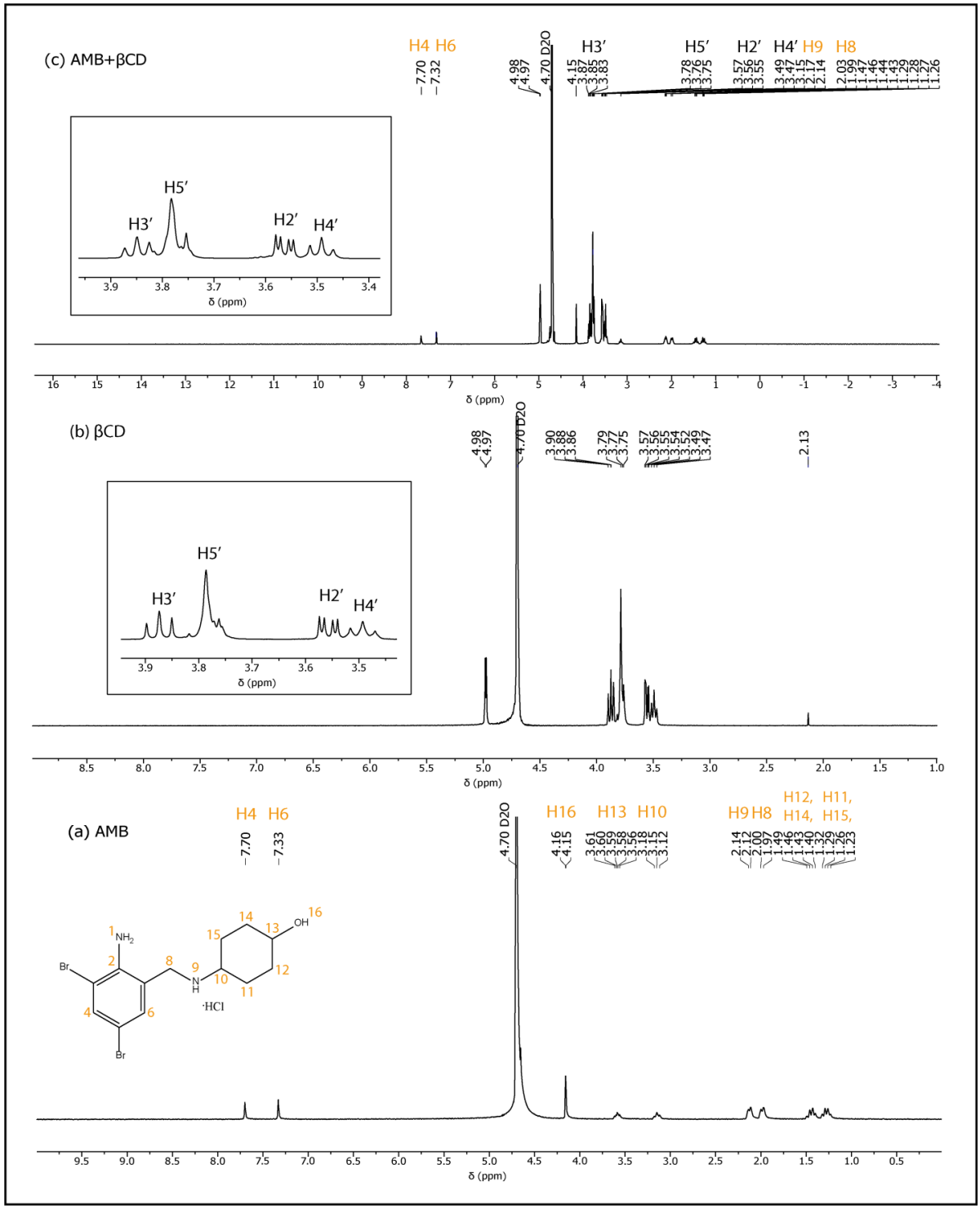

Fig. S10: ^{1}H-NMR spectral data for (a) Free AMB (b) Free βCD (c) AMB+βCD Inclusion Complex

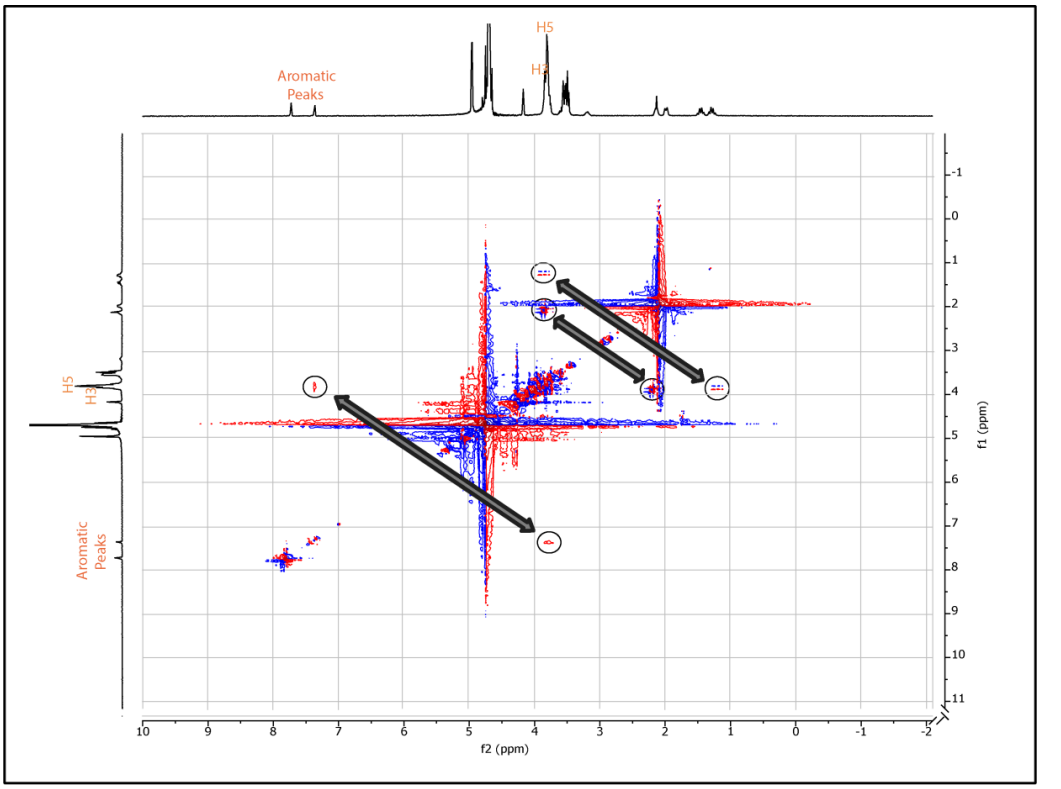

Figure S11: 2D-NMR of AMB+αCD inclusion complex

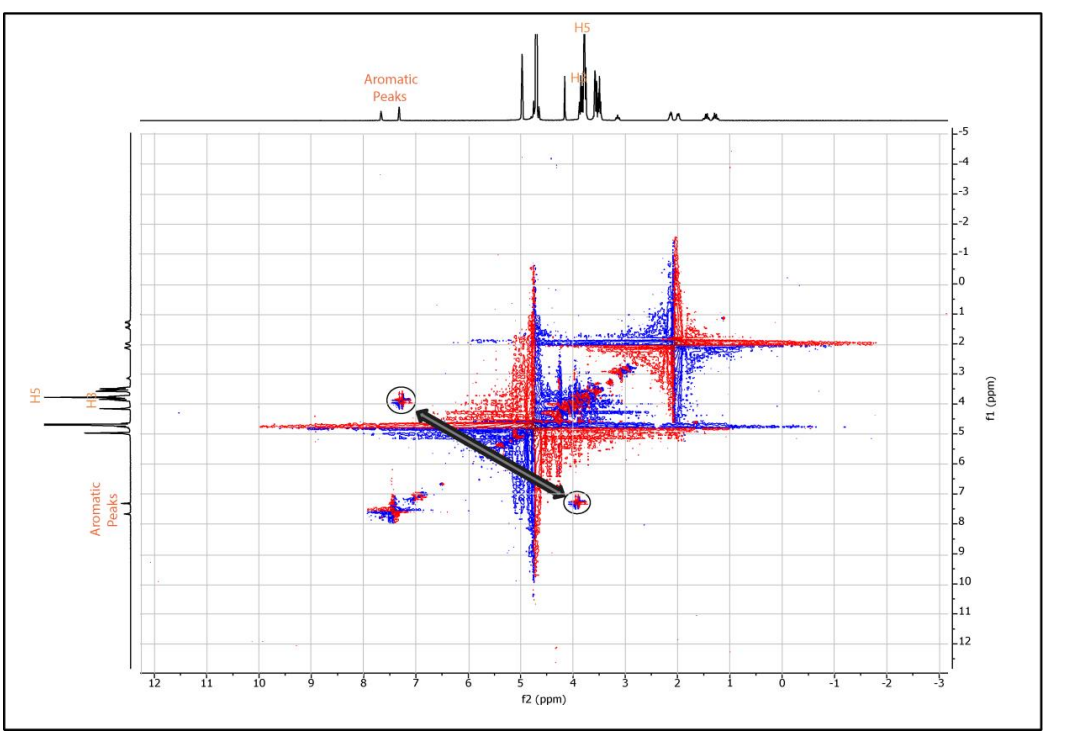

Figure S12: 2D-NMR of AMB+βCD inclusion complex

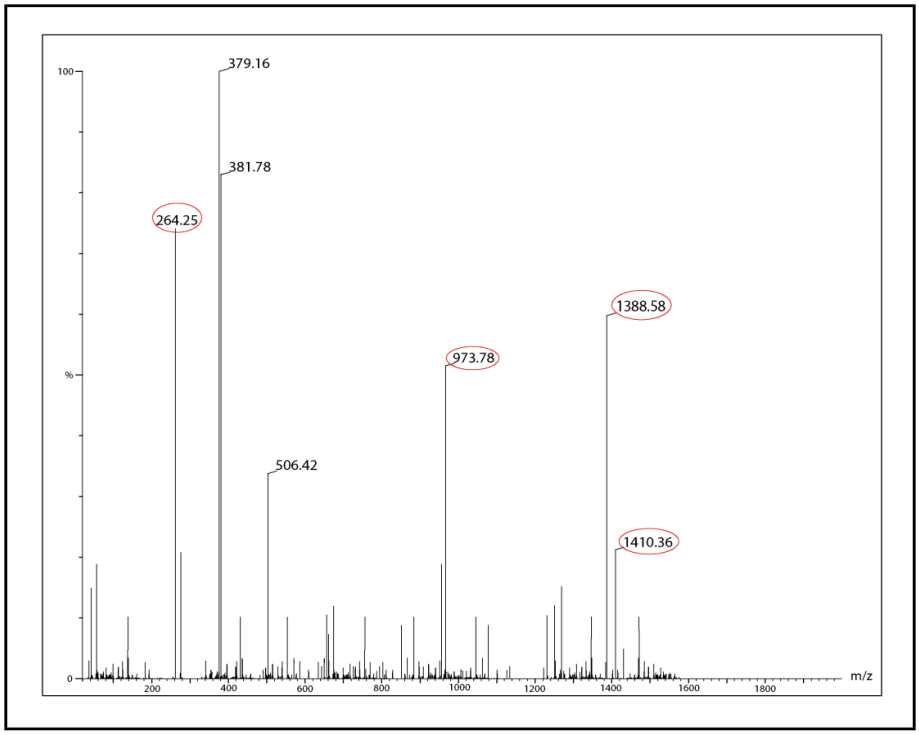

Figure S13: ESI-MS spectra of AMB+αCD inclusion complex

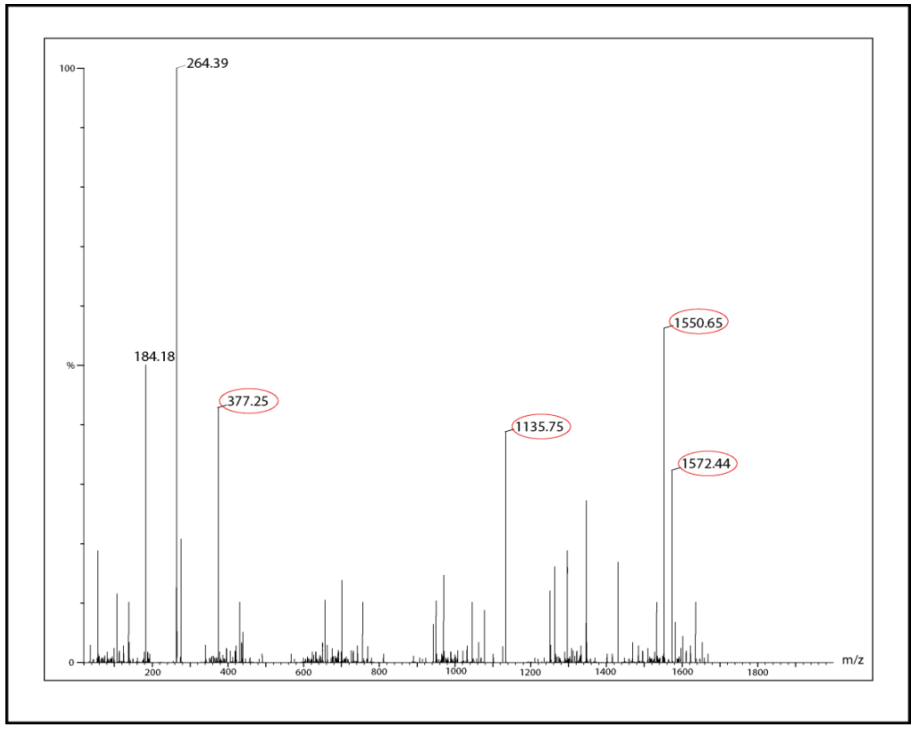

Figure S14: ESI-MS spectra of AMB+βCD inclusion complex

SCHEMES

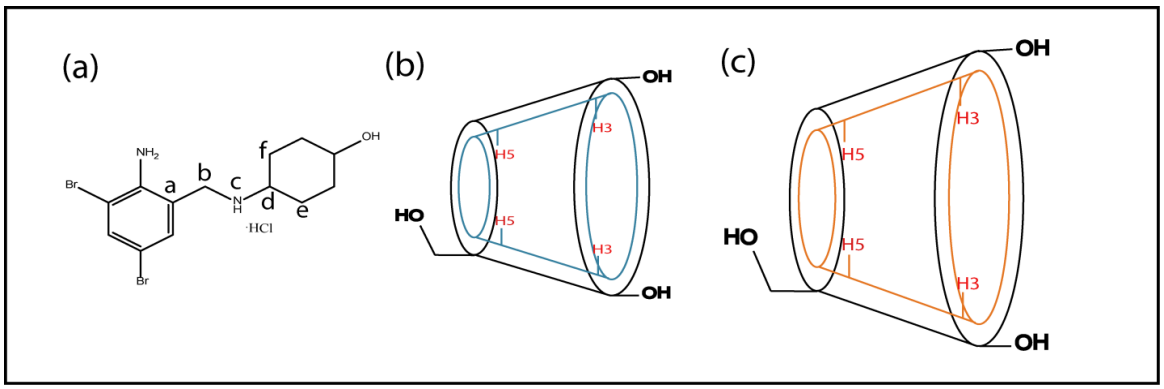

Scheme 1: Two dimensional structures of (a) Ambroxol hydrochloride (b) α-cyclodextrin (c) β-cyclodextrin

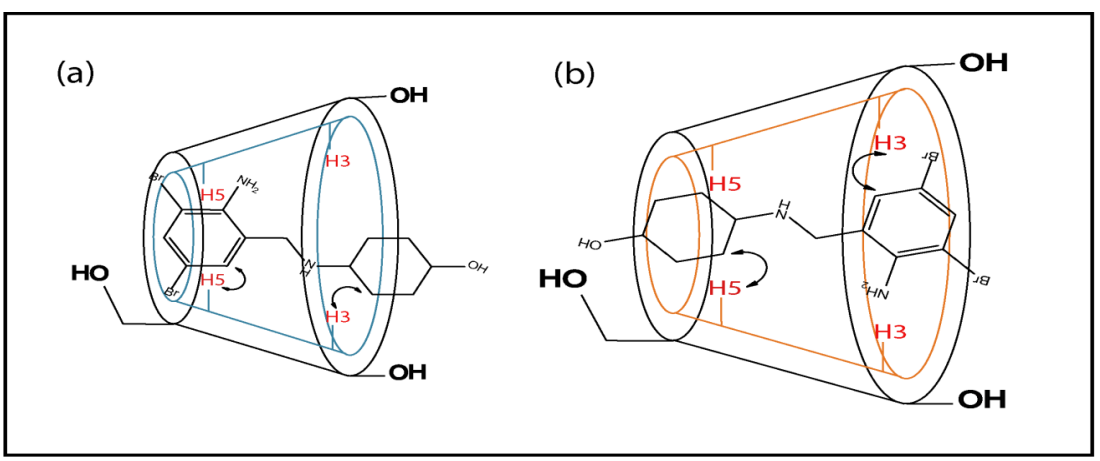

Scheme 2: Plausible inclusion mechanism of (a) AMB+αCD inclusion complex (b) AMB+βCD inclusion complex predicted by ^{1}H-NMR and 2D-NMR